# Perilipin regulates the thermogenic actions of norepinephrine in brown adipose tissue

**Sandra C. Souza,[1,*] Marcelo A. Christoffolete,[1,†] Miriam O. Ribeiro,[§] Hideaki Miyoshi,[*,**] Katherine J. Strissel,[*] Zlatina S. Stancheva,[*] Nicole H. Rogers,[*] Tara M. D'Eon,[*,††] James W. Perfield, II,[*] Hitomi Imachi,[*,§§] Martin S. Obin,[*] Antonio C. Bianco,[2,†] and Andrew S. Greenberg[2,*]**

Jean Mayer United States Department of Agriculture-Human Nutrition Research Center on Aging at Tufts University,* Boston, MA; Brigham and Women's Hospital and Harvard Medical School,† Boston, MA; Biological and Health Science Center,§ Mackenzie Presbyterian University, São Paulo, Brazil; Hokkaido University Graduate School of Medicine,** Sapporo, Japan; Elixir Pharmaceuticals,†† Cambridge, MA; and Kagawa Medical University,§§ Kagawa, Japan

**Abstract In response to cold, norepinephrine (NE)-induced triacylglycerol hydrolysis (lipolysis) in adipocytes of brown adipose tissue (BAT) provides fatty acid substrates to mitochondria for heat generation (adaptive thermogenesis). NE-induced lipolysis is mediated by protein kinase A (PKA)-dependent phosphorylation of perilipin, a lipid droplet-associated protein that is the major regulator of lipolysis. We investigated the role of perilipin PKA phosphorylation in BAT NE-stimulated thermogenesis using a novel mouse model in which a mutant form of perilipin, lacking all six PKA phosphorylation sites, is expressed in adipocytes of perilipin knockout (Peri KO) mice. Here, we show that despite a normal mitochondrial respiratory capacity, NE-induced lipolysis is abrogated in the interscapular brown adipose tissue (IBAT) of these mice. This lipolytic constraint is accompanied by a dramatic blunting (~70%) of the in vivo thermal response to NE. Thus, in the presence of perilipin, PKA-mediated perilipin phosphorylation is essential for NE-dependent lipolysis and full adaptive thermogenesis in BAT. In IBAT of Peri KO mice, increased basal lipolysis attributable to the absence of perilipin is sufficient to support a rapid NE-stimulated temperature increase (~3.0°C) comparable to that in wild-type mice. This observation suggests that one or more NE-dependent mechanism downstream of perilipin phosphorylation is required to initiate and/or sustain the IBAT thermal response.**—Souza, S. C., M. A. Christoffolete, M. O. Ribeiro, H. Miyoshi, K. J. Strissel, Z. S. Stancheva, N. H. Rogers, T. M. D'Eon, J. W. Perfield, II, H. Imachi, M. S. Obin, A. C. Bianco, and A. S. Greenberg. **Perilipin regulates the thermogenic actions of norepinephrine in brown adipose tissue. *J. Lipid Res.* 2007.** 48: **1273–1279.**

**Supplementary key words** norepinephrine-induced thermal response • protein kinase A-stimulated lipolysis • brown adipocytes

*Manuscript received 29 January 2007 and in revised form 15 March 2007.*

*Published, JLR Papers in Press, March 30, 2007.*
*DOI 10.1194/jlr.M700047-JLR200*

Obesity has become a major health issue in Western and developing countries as a result of increased energy intake from unhealthy diets and a sedentary lifestyle corresponding to decreased energy expenditure (1). One of the key manifestations of the metabolic imbalance resulting from obesity is the increased rate of FFA storage and release by adipose tissue. Increased FFA turnover is thought to be a critical factor for the development of insulin resistance, diabetes, and obesity-associated metabolic complications (2). In response to catecholamine stimulation, FFAs are released from triacylglycerol (TAG) stored within lipid droplets in white adipose tissue (WAT) and brown adipose tissue (BAT). In WAT, catecholamine-stimulated lipolysis provides fatty acids as a fuel to peripheral tissues during times of energy need. In interscapular brown adipose tissue (IBAT) of human newborns and rodents, catecholamine-stimulated lipolysis provides fatty acids for heat production in response to cold exposure or overfeeding, a process called adaptive thermogenesis (3). More specifically, norepinephrine (NE) is the endogenous mediator of adaptive thermogenesis (4, 5). Increased understanding of BAT metabolism may be critical for providing new approaches to treatments for obesity and associated disorders.

In adaptive thermogenesis, fatty acids activate uncoupling protein-1 (UCP1) in the mitochondria, producing heat instead of ATP as an end product of oxidative

Abbreviations: ATGL, adipose tissue triacylglycerol lipase; BAT, brown adipose tissue; HSL, hormone-sensitive lipase; IBAT, interscapular brown adipose tissue; NE, norepinephrine; Peri A, perilipin isoform A; Peri KO, perilipin knockout; PKA, protein kinase A; TAG, triacylglycerol; UCP1, uncoupling protein-1; WAT, white adipose tissue; WT, wild-type.

[1] S. C. Souza and M. A. Christoffolete contributed equally to this work.

[2] To whom correspondence should be addressed.

e-mail: abianco@partners.org (A.C.B.); andrew.greenberg@tufts.edu (A.S.G.).

phosphorylation (6, 7). IBAT thermogenesis is initiated by the binding of NE (released from sympathetic nerve endings) to β-adrenergic receptors coupled to an adenylyl cyclase system (8). In white adipocytes, the increase in cAMP activates cAMP dependent protein kinase A (PKA), which phosphorylates two major substrates: hormone-sensitive lipase (HSL) and perilipins (9). Perilipins are phosphoproteins located on the surface of the lipid droplet where lipolysis occurs (10). In the basal state, perilipins prevent the action of lipases and subsequently the hydrolysis of TAG (11–13). Upon phosphorylation by PKA, perilipins function as facilitators of lipolysis, orchestrating the action of lipases such as HSL and adipose tissue triacylglycerol lipase (ATGL), a recently discovered hormonally regulated lipase proposed to attenuate basal lipolysis and to enhance catecholamine-stimulated lipolysis (14, 15). Although perilipin's role in white adipocytes is well defined, little is known about the role of perilipin and PKA-induced phosphorylation of perilipin in brown adipocytes and the resulting effects on thermogenesis.

Perilipin isoform A (Peri A) is the major isoform expressed in white and brown adipocytes and has six PKA consensus sites. Recently, we demonstrated that mutating serine residues to alanines in all six sites completely abrogates cAMP-stimulated lipolysis in several in vitro cell systems (16, 17). Despite the existence of numerous published studies in this area of investigation (16–21), no experiments have ever been performed to examine the role of PKA-dependent phosphorylation of Peri A in regulating TAG lipolysis and adaptive thermogenesis in BAT in vivo.

In this study, we used two animal models of altered perilipin function to investigate the requirement for perilipin and its PKA-dependent phosphorylation in NE-induced BAT thermogenesis, a direct measure of adaptive thermogenesis. We generated a perilipin knockout (Peri KO) mouse and a novel mouse model in which a mutant perilipin transgene lacking all six PKA phosphorylation sites was expressed in adipocytes of the Peri KO mouse (Peri AKOΔ1-6) (17). Our thermogenic studies revealed that when perilipin is present, its PKA-dependent phosphorylation is crucial for lipolysis and normal adaptive thermogenesis in vivo. Interestingly, studies in Peri KO mice suggest that adaptive thermogenesis in vivo requires NE-dependent mechanisms in addition to enhanced lipolysis.

## RESEARCH DESIGN AND METHODS

### Chemicals and antibodies

Reagents and a mouse monoclonal antibody specific for the Flag peptide were purchased from Sigma Chemical Co. (St. Louis, MO). L-(−)-NE-(+) bitartrate was purchased from Calbiochem (La Jolla, CA). A rabbit polyclonal anti-perilipin antibody and a rabbit polyclonal anti-HSL antibody were generated as described previously (13). An ATGL antibody was generated (QCB, Hopkinton, MA) using the peptide CTNVAFPPDALRMRAPAS and was subsequently affinity-purified for use in Western blotting (1:2,000). The goat anti-UCP1 polyclonal antibody was purchased from Santa Cruz Biotechnology (Santa Cruz, CA) and used according to the instructions.

### Peri KO and Peri AKOΔ1-6 mice

Peri KO mice were generated by targeted disruption of the perilipin gene, which replaced exon 3 (nucleotides 3,515 to 3,887) with a neomycin cassette, thereby disrupting the coding of all known perilipin mRNAs. Peri KO mice were backcrossed for 10 generations to C57BL/6 mice (Harlan, Indianapolis, IN). We generated a mouse Peri AΔ1-6 cDNA with a Flag tag at the C terminus using a standard PCR method (17). This cDNA was then ligated into a *Sma*I site of pBluescript SK vector containing the aP2 enhancer/promoter region, the SV40 small tumor antigen splice site, and a polyadenylation signal sequence (a gift of Dr. B. M. Spiegelman) (22). A fragment containing the entire aP2-Peri A-Flag transgene was microinjected into fertilized eggs of C57BL/6 mice. Transgenic mice expressing the Peri AΔ1-6 transgene almost exclusively in IBAT were obtained. These transgenic mice were mated with backcrossed Peri KO mice to generate the Peri AKOΔ1-6 mice (hemizygous for the transgene) used in these studies (17). All mice were housed at room temperature, fed ad libitum, with water provided at all times. Experiments were performed between 16 and 18 weeks of age.

### Isolation of mitochondria and oxygen consumption

Mitochondria from BAT and whole liver were isolated by homogenization followed by differential centrifugation as described previously (23). Oxygen consumption was measured with a Clark-type polarographic oxygen probe in a biological oxygen monitor system (YSI 5300A; Yellow Spring Instrument Co., Yellow Springs, OH) using succinate (5 mM) as the substrate in the absence and presence of ADP (100 μM). Data are expressed as nanomoles of oxygen consumed per milligram of protein per minute. The protein concentration of the mitochondrial suspensions was determined using a bicinchoninic acid kit (Bio-Rad, Hercules, CA).

### IBAT and core thermal response to NE infusion

IBAT and core thermal response to NE were determined as described previously (24). Briefly, animals were anesthetized with a mixture of urethane (560 mg/kg intraperitoneally) and chloralose (38 mg/kg intraperitoneally) on the morning of the experiment. Mice were kept warm (30°C) with a heating pad through the course of the experiment. A polyethylene (P-50) cannula was inserted into the left jugular vein and later used for NE infusion. IBAT temperatures were measured using a precalibrated thermistor probe (YSI 427; Yellow Springs Instrument Co.) secured under the brown fat pad. Core temperature was measured with a colonic probe (YSI 423; Yellow Springs Instrument Co.). The probes were connected to a high-precision thermometer (YSI Precision 4000A Thermometer; Yellow Springs Instrument Co.). Core temperature and IBAT temperatures were monitored during a period of 10 min to obtain a stable baseline, followed by NE infusion (1,075 pmol/min) using an infusion pump (Harvard model 2274; Harvard Apparatus, Holliston, MA) (0.459 μl/min for 30 min). Raw data were plotted over time and expressed in terms of maximum change in ΔIBAT temperature (°C).

### Histology and TAG content

Hematoxylin and eosin staining was performed on paraffin sections of IBAT from wild-type (WT), Peri AKOΔ1-6, and Peri KO mice. For lipid analysis, 20 mg of IBAT tissue was homogenized in 1 ml of hexane-isopropanol (3:2). After spinning at 1,000 rpm, extraction was repeated and solvent-containing lipid was dried at room temperature. Lipids were then dissolved in 500 μl of isopropanol, and TAG content was measured using triglyceride reagent (Sigma). TAG is expressed in micromoles

per milligram of tissue and represents the average of five mice per group.

### Western analysis

Adipose tissue proteins were extracted as described previously (25) and quantified using the BCA protein assay (Pierce Biotechnology, Inc., Rockford, IL). Total lysates (20 μg/sample) were separated by 10% SDS-PAGE, transferred electrophoretically to nitrocellulose membranes, and blotted as described previously (13).

### Brown adipocyte isolation and lipolysis

Brown adipocytes were isolated using collagenase and centrifugation of pooled IBAT depots as described previously (26) with minor modifications. Cleaned BAT was minced and digested in Krebs-Ringer phosphate buffer containing 1% BSA and 2 mg/ml collagenase. Buffer containing cells and tissue fragments was filtered through a 70 μm filter. Collagenase was removed by centrifugation at 2,200 rpm and infranatant removal using a spinal needle (BD Medical Systems, Franklin Lakes, NJ). Brown adipocytes from WT (50,000 cells), Peri AKOΔ1-6 (70,000 cells), or Peri KO (70,000 cells) mice were divided into aliquots in triplicate, and lipolysis under basal (200 nM phenyl isopropyl adenosine) and stimulated (200 nm phenyl isopropyl adenosine + 10 μM NE) conditions was measured. Lipolytic rate was assessed as glycerol released into the medium over 1 h using a Free Glycerol Determination kit (Sigma) (13). Lipolysis is expressed relative to milligrams of lipid. Free fatty acids were determined using an acyl-CoA oxidase-based colorimetric kit (NEFA-C; WAKO Pure Chemicals, Osaka, Japan) (25).

### Quantitative PCR

Total RNA was extracted from IBAT using a commercial kit (RNeasy lipid tissue; Qiagen, Inc., Valencia, CA). RNA was quantified by RiboGreen Quantitation Assay (Molecular Probes, Eugene, OR), and cDNA was synthesized from 1 μg of total RNA (Reverse Transcription System; Promega, Madison, WI). Real-time PCR was performed in triplicate on an ABI PRISM® 7700 in a total volume of 20 μl using SYBR® Green PCR Master Mix (Applied Biosystems, Foster City, CA). Primers were designed using Primer Express (sequences available on request). Data were analyzed by the comparative critical threshold method (27) and normalized to an endogenous control gene (18S rRNA). Assuming that primer efficiencies are similar, percentage differences were calculated by the formula $2^{-\Delta\Delta Ct}$ where ΔΔCt is the difference in threshold cycles for the target and control samples.

### Statistical analysis

Results are presented as mean values ± SEM. Paired or unpaired *t*-tests were performed using Microsoft Excel. $P \leq 0.05$ was considered significant.

## RESULTS

### Peri AKOΔ1-6 expression is higher in IBAT

A construct containing 5.4 kb of the adipocyte-specific promoter/enhancer aP2 driving the expression of a C-terminal Flag-tagged Peri A cDNA, carrying serine-to-alanine mutations in all six PKA sites, was used to generate a transgenic mouse line (**Fig. 1A**). These transgenic mice were bred with Peri KO mice, thus generating the Peri AKOΔ1-6 mice with targeted adipose Peri AΔ1-6 expression. The mice were viable, born at the expected Mendelian frequency, and exhibited normal reproduction. Body weight and linear growth determined by nasal-anal length were similar among WT, Peri AKOΔ1-6, and Peri KO mice (data not shown). The tissue specificity of the transgene expression was assessed by Western blot analysis of Peri AKOΔ1-6 Flag protein (Fig. 1B). Peri AKOΔ1-6 Flag protein expression was restricted to adipose tissue; no signal was detected in liver, spleen, or muscle of the Peri AKOΔ1-6 mice. Peri AKOΔ1-6 Flag protein expression in these mice was highest in IBAT, with only a faint band observed in inguinal, perirenal, and epididymal WAT depots. This uneven Peri AKOΔ1-6 expression resulted in WAT depots that were larger than those present in the Peri KO mice but smaller than those in control mice (data not shown). IBAT depot weight from Peri AKOΔ1-6 mice tended to be more similar to that of WT mice, whereas the depot weight was reduced ($P \leq 0.01$) in Peri KO mice (WT, 0.15 ± 0.05 g; Peri AKOΔ1-6, 0.16 ± 0.01 g; Peri KO, 0.10 ± 0.01 g; n = 5). As observed in white adipocytes, the absence of perilipin in IBAT is associated with the expression of adipose-differentiation related protein, which stabilizes the lipid droplets (Fig. 1C) (13, 28). The levels

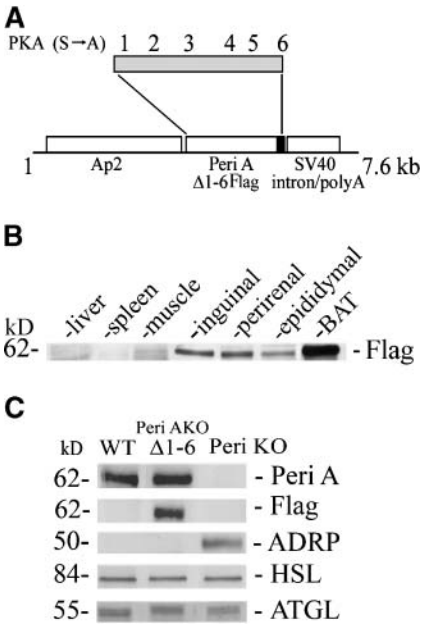


**Fig. 1.** Peri AKOΔ1-6 protein is preferentially expressed in interscapular brown adipose tissue (IBAT) of Peri AKOΔ1-6 mice. A: Scheme of the transgenic construct showing the mouse aP2 promoter/enhancer, the cDNA for perilipin isoform A (Peri A) Δ1-6 protein kinase A (PKA) Flag-tagged at the C terminus, and the SV40 intron/poly(A) signal. These transgenic mice were mated with perilipin knockout (Peri KO) mice to generate the Peri AKOΔ1-6 mice used in these studies. B: Western blotting analysis of protein lysates from Peri AKOΔ1-6 mouse tissues using antibody recognizing the Flag epitope. C: Western blotting of protein lysates collected from IBAT of wild-type (WT), Peri AKOΔ1-6, and Peri KO mice immunoblotted with antibodies recognizing Peri A, the Flag epitope ligated to Peri AΔ1-6, adipose-differentiation related protein (ADRP), hormone-sensitive lipase (HSL), and adipose tissue triacylglycerol lipase (ATGL).

of the protein lipases HSL and ATGL were not significantly different among WT, Peri AKOΔ1-6, and Peri KO mice (Fig. 1C).

### Morphology, histology, and TAG content in IBAT of Peri AKOΔ1-6 mice

Investigation of IBAT depots from 18 week old mice revealed that IBAT of Peri AKOΔ1-6 mice was slightly larger (**Fig. 2A**), contained larger lipid droplets (Fig. 2B), and had 67% more TAG content than that in WT mice (Fig. 2C). In contrast, IBAT of Peri KO mice was darker (Fig. 2A), displayed smaller lipid droplets (Fig. 2B), and exhibited 47% less TAG content (Fig. 2C) than that in WT mice.

### NE-induced thermal response is blunted in IBAT of Peri AKOΔ1-6 mice

Because the expression of perilipin A or Δ1-6-mutated perilipin was similar in IBAT of WT and Peri AKOΔ1-6 mice, respectively, we used the latter model to elucidate the in vivo role of PKA-dependent perilipin phosphorylation in IBAT-dependent adaptive thermogenesis. To evaluate IBAT thermogenesis directly, we measured changes in the temperature of the IBAT depot in response to a 30 min constant intravenous NE infusion (1.1 pmol/min) in anesthetized mice. In WT mice, NE infusion elicited a rapid and progressive increase in IBAT and core temperatures, which reached maxima of ~3.0°C and 1.5°C, respectively (**Fig. 3A**, **B**). Notably, the increase in core temperature had a delay of ~10 min compared with the IBAT thermal profile, confirming the expected temperature gradient (24). Remarkably, the IBAT thermal profile was indistinguishable in the Peri KO mice compared with WT mice, whereas in Peri AKOΔ1-6 mice an ~70% reduction was observed (Fig. 3A). These changes are physiologically relevant, as the core temperature in the Peri AKOΔ1-6 mice also failed to increase accordingly (Fig. 3B). These findings demonstrate a clear deficit in the Peri AKOΔ1-6 IBAT-dependent adaptive thermogenesis.

### Mitochondrial respiration and UCP1 levels are normal in Peri AKOΔ1-6 IBAT

To test whether the deficit observed in the Peri AKOΔ1-6 IBAT is related to a mitochondrial dysfunction, we first analyzed the UCP1 protein levels in both animal models by Western blotting and found them to be similar to WT levels (**Fig. 4A**). Next, we measured IBAT mRNA levels of transcripts involved in β-oxidation (i.e., mitochondrial carnitine palmitoyltransferase 1 and 2, carnitine/acylcarnitine translocase, 3-ketoacyl-CoA thiolase B) and found no differences among the three groups of animals (Fig. 4B). Functional mitochondrial studies were performed by analyzing oxygen consumption of isolated IBAT mitochondria in the presence of 5 mM succinate as substrate (stage 2) and in the presence of 100 μM ADP (stage 3) (23). The profiles revealed no differences in IBAT mitochondrial oxygen consumption during stages 2 and 3 of respira-

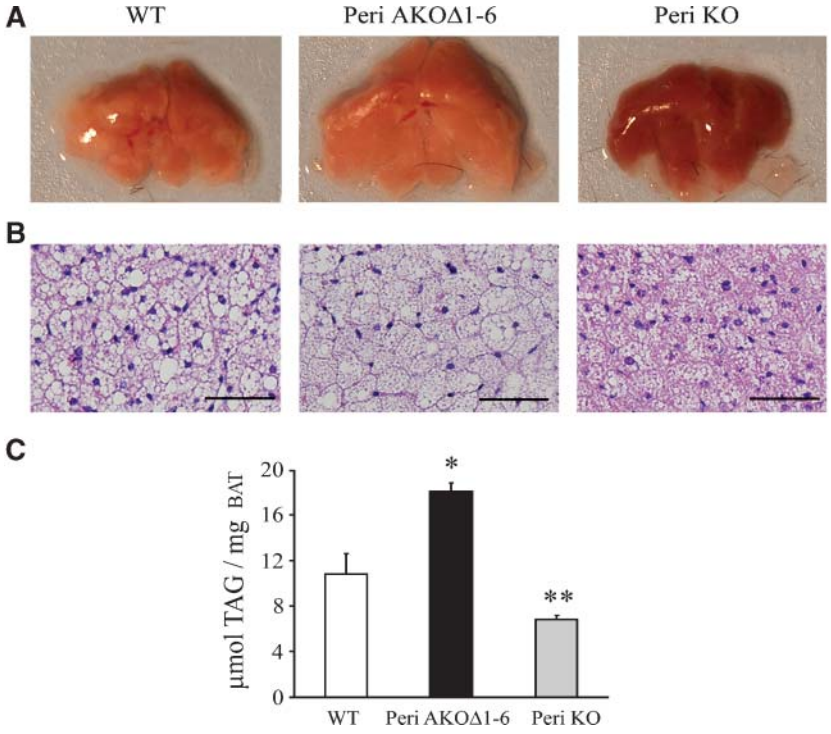


**Fig. 2.** Altered lipid deposition in IBAT of Peri AKOΔ1-6 and Peri KO mice. A: Gross observation of the brown adipose tissue (BAT) from WT, Peri AKOΔ1-6, and Peri KO mice. B: Histological hematoxylin and eosin-stained sections of fixed BAT tissues from these mice. Bars = 50 μm. C: Triacylglycerol (TAG) content determined from total lipid extracted from IBAT sections, normalized by tissue weight. Data are expressed as means ± SEM of five mice/group. * $P \leq 0.01$; ** $P \leq 0.05$ versus WT mice.

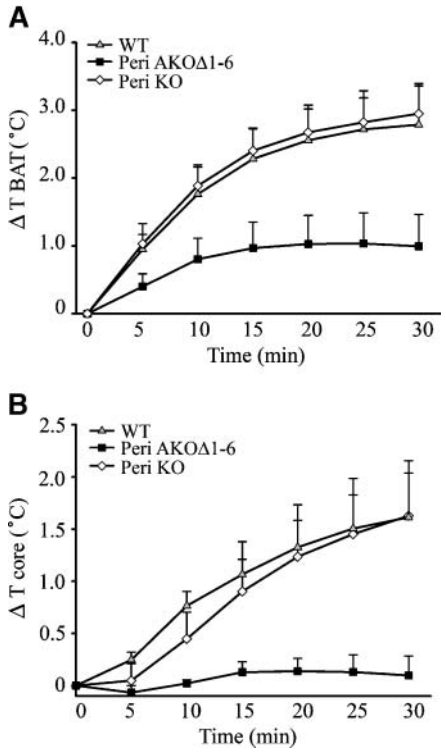


**Fig. 3.** Norepinephrine (NE)-induced thermal response is dramatically blunted in IBAT of Peri AKOΔ1-6 mice and normal in IBAT of Peri KO mice. IBAT (A) and core (B) temperatures (T) were measured in anesthetized mice before (baseline) and during NE infusion at a rate of 1,075 pmol/min. The data represent maximal responses above baseline every 5 min over a period of 30 min of NE infusion. Values are expressed as means ± SEM of four mice/group.

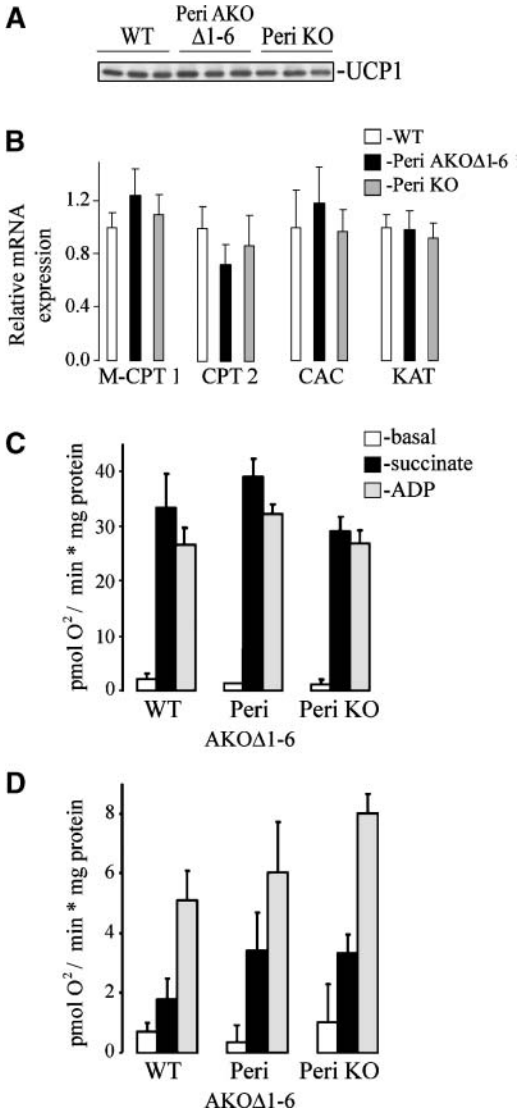


**Fig. 4.** Mitochondrial oxygen consumption is unaffected in IBAT of Peri AKOΔ1-6 mice. A: Western blotting for uncoupling protein-1 (UCP1) from IBAT of WT, Peri AKOΔ1-6, and Peri KO mice. Each lane represents an individual mouse. B: mRNA expression of genes selective for fatty acid oxidation in IBAT [mitochondrial carnitine palmitoyltransferase 1 and 2 (M-CPT1, CPT2), carnitine/acylcarnitine translocase (CAC), and 3-ketoacyl-CoA thiolase B (KAT)] (n = 5/group). C, D: Oxygen consumption of isolated mitochondria from IBAT (C) and liver (D) of WT, Peri AKOΔ1-6, and Peri KO mice was measured using succinate (5 mM) as substrate in the absence and presence of ADP (100 μM). Data are expressed as picomoles of oxygen consumed per milligram of protein per minute. Results represent means ± SEM of two experiments performed in triplicate.

tion among WT, Peri AKOΔ1-6, and Peri KO mice (Fig. 4C). It is notable that no further increase in oxygen consumption was observed after the addition of ADP, reflecting the uncoupled state of IBAT mitochondria (29). As a control, oxygen consumption in mitochondria isolated from liver was studied under similar conditions and found to be comparable in WT, Peri AKOΔ1-6, and Peri KO mice, as expected (23), including increased oxygen consumption at stage 3 of mitochondrial respiration (Fig. 4D).

### Lipolysis in isolated brown adipocytes

A 2-fold increase in glycerol and FFA release was observed in isolated WT brown adipocytes treated with 10 μm NE for 1 h (**Fig. 5A**, **B**). In contrast, NE-stimulated lipolysis was abrogated in Peri AKOΔ1-6 brown adipocytes (Fig. 5A, B), confirming the impaired cAMP-stimulated lipolysis observed in similar cell models of Peri AKOΔ1-6 expression (16, 17). Basal lipolysis was also reduced, presumably reflecting the abrogation of basal levels of perilipin phosphorylation. Isolated brown adipocytes of Peri KO mice exhibited an increased basal glycerol and fatty acid release rate that was not stimulated further by exposure to NE (Fig. 5A, B).

## DISCUSSION

This study provides the first in vivo evidence that perilipin phosphorylation is required for normal lipolysis and adaptive thermogenesis in BAT. To explore the role of perilipin PKA phosphorylation sites in BAT thermogenesis, we developed a novel model (the Peri AKOΔ1-6 mouse), which expresses a mutant perilipin transgene lacking all six PKA phosphorylation sites in adipocytes of

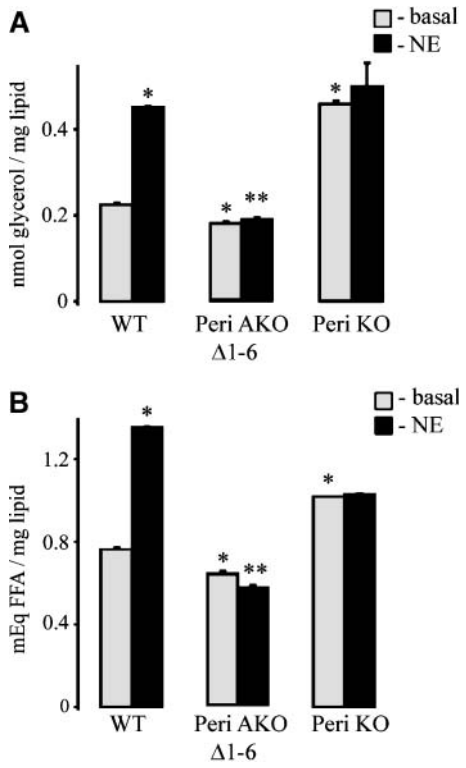


**Fig. 5.** Peri AKOΔ1-6 and Peri KO isolated brown adipocytes are unresponsive to NE-stimulated lipolysis. Isolated brown adipocytes were treated with phenyl isopropyl adenosine (basal) or with NE (10 μM) for 1 h, after which medium was collected and assayed for glycerol (A) and FFA (B). Results represent means ± SEM of two experiments performed in triplicate. * $P \leq 0.05$ versus the basal value of WT mice; ** $P \leq 0.001$ versus NE of WT mice.

Peri KO mice (Fig. 1). In these mice, perilipin is expressed on the lipid droplets of brown adipocytes and the rates of basal lipolysis are low, reflecting perilipin's actions as a barrier to lipases in the nonphosphorylated state (Fig. 5A, B) (11, 13, 14, 16, 17, 28). However, Δ1-6 perilipin cannot be phosphorylated by PKA, thereby precluding NE-induced lipolysis as well (Fig. 5A, B) (16, 17). Thus, the expression of Δ1-6 perilipin results in low rates of both basal and PKA-stimulated lipolysis in isolated brown adipocytes of Peri AKOΔ1-6 mice (Fig. 5). These results confirm and extend our initial in vitro observations using differentiated brown preadipocytes from Peri AKOΔ1-6 (16, 17).

Using a direct method to assess the actions of NE to increase thermogenesis, we demonstrate that NE-induced IBAT thermogenesis is dramatically impaired in Peri AKOΔ1-6 mice and that this impairment is attributable to defective PKA-dependent lipolytic activation. We demonstrate that in WT animals NE infusion increased IBAT temperature by ~3.0°C and subsequently caused an increase in core temperature. In contrast, the thermal increase observed in IBAT of Peri AKOΔ1-6 was limited to ~1.0°C, with no detectable change in core temperature (Fig. 3A, B). In view of the fact that mitochondrial function is preserved and UCP1 levels are normal in Peri AKOΔ1-6 mice (Fig. 4), these results demonstrate the critical role of perilipin phosphorylation and PKA-dependent lipolysis in IBAT thermogenesis.

The normal thermal response to NE infusion observed in Peri KO mice (Fig. 3A, B) was intriguing, given the demonstrated requirement of perilipin for PKA-stimulated lipolysis in adipocytes (28, 30). Indeed, in this study, NE treatment failed to induce TAG hydrolysis above constitutive levels in brown adipocytes from Peri KO mice (Fig. 5). However, because of the absence of perilipin, basal (constitutive) lipolysis in BAT of Peri KO mice was increased, achieving levels comparable to PKA-stimulated lipolysis in WT mice (Fig. 5). Thus, basal rates of TAG hydrolysis in IBAT of Peri KO mice provide sufficient fatty acids to fully support NE-stimulated thermogenesis. Our demonstration of normal adaptive thermogenesis in Peri KO mice is reflected in the normal capacity of fed mice to maintain core body temperature in response to cold exposure (30). Interestingly, in the absence of NE treatment, the increased rate of constitutive TAG hydrolysis in Peri KO mice is not sufficient to induce BAT thermogenesis, suggesting that NE-dependent cell biological mechanisms "downstream" of, or in addition to, lipolysis are required for NE-induced thermogenesis.

In conclusion, the blunted IBAT thermogenic response to NE detected in Peri AKOΔ1-6 mice indicates that PKA-mediated perilipin phosphorylation and the subsequent TAG hydrolysis are critical for adaptive thermogenesis in brown adipocytes. In addition, our studies also provide evidence for the existence of other equally critical NE-dependent but perilipin-independent mechanisms that must be activated to initiate and sustain the IBAT thermal response.

The authors thank Donald Smith and Andrea A. Pinilla for providing excellent animal experiment support and expertise. The authors thank Dr. Bruce M. Spiegelman for providing the aP2 construct. H.M. thanks Prof. Takao Koike for continued support and mentorship. M.O.R. was the recipient of a grant from MackPesquisa, Brazil. This work was supported by National Institutes of Health Grant DK-50647 and U.S. Department of Agriculture-Agricultural Research Service Cooperative Agreement 58 1950-7-707 (to A.S.G.), by the Center for Digestive Disease Research on Absorptive and Secretory Processes (National Institutes of Health Grant P30 DK-34928), by the Boston Obesity Nutrition Research Center (National Institutes of Health Grants DK-46200 and P30 DK-46200 to K.J.S.), by the American Diabetes Association Grant 1-06-RA-96 (to M.S.O.), and by the Tufts Center for Neuroscience Research Grant P30 NS-047243.

## REFERENCES

1. Mokdad, A., E. Ford, B. Bowman, W. Dietz, F. Vinicor, V. Bales, and J. Marks. 2003. Prevalence of obesity, diabetes, and obesity-related health-risk factors, 2001. *J. Am. Med. Assoc.* **289:** 76–79.
2. Roden, M., T. Price, G. Perseghin, K. Petersen, D. Rothman, G. Cline, and G. Shulman. 1996. Mechanism of free fatty acid-induced insulin resistance in humans. *J. Clin. Invest.* **97:** 2859–2865.
3. Robidoux, J., T. L. Martin, and S. Collins. 2004. Beta-adrenergic receptors and regulation of energy expenditure: a family affair. *Annu. Rev. Pharmacol. Toxicol.* **44:** 297–323.

4. Thomas, S., and R. Palmitier. 1997. Thermoregulatory metabolic phenotypes of mice lacking noradrenaline and adrenaline. *Nature.* **287:** 94–97.
5. Bachman, E., H. Dhillon, C. Zhang, S. Cinit, A. Bianco, B. Koblka, and B. Lowell. 2002. Beta AR signaling required for diet-induced thermogenesis and obesity resistance. *Science.* **297:** 843–845.
6. Kozak, L., and M-E. Harper. 2000. Mitochondrial uncoupling proteins in energy expenditure. *Annu. Rev. Nutr.* **20:** 339–363.
7. Nicholls, D. G., and R. M. Locke. 1984. Thermogenic mechanisms in brown fat. *Physiol. Rev.* **64:** 1–64.
8. Cannon, B., and J. Nedergaard. 2004. Brown adipose tissue: function and physiological significance. *Physiol. Rev.* **84:** 277–359.
9. Belfrage, P., G. Fredrikson, H. Olsson, and P. Stralfors. 1982. Hormonal regulation of adipose tissue lipolysis by reversible phosphorylation of hormone-sensitive lipase. *Prog. Clin. Biol. Res.* **102:** 213–223.
10. Greenberg, A. S., J. J. Egan, S. A. Wek, N. B. Garty, E. J. Blanchette-Mackie, and C. Londos. 1991. Perilipin, a major hormonally regulated adipocyte-specific phosphoprotein associated with the periphery of lipid storage droplets. *J. Biol. Chem.* **266:** 11341–11346.
11. Brasaemle, D., B. Rubin, I. Harten, J. Gruia-Gray, A. Kimmel, and C. Londos. 2000. Perilipin A increases triacylglycerol storage by decreasing the rate of triacylglycerol hydrolysis. *J. Biol. Chem.* **275:** 38486–38493.
12. Souza, S., L. Moitoso de Vargas, M. Yamamato, P. Line, M. Franciosa, L. Moss, and A. Greenberg. 1998. Overexpression of perilipin A and B blocks the ability of tumor necrosis factor to increase adipocyte lipolysis in 3T3-L1 adipocytes. *J. Biol. Chem.* **273:** 24665–24669.
13. Souza, S., K. Muliro, L. Liscum, P. Lien, Y. Yamamoto, J. Schaffer, G. Dallal, X. Wang, F. Kraemer, M. Obin, et al. 2002. Modulation of hormone-sensitive lipase and protein kinase-A-mediated lipolysis by perilipin A in an adenoviral reconstituted system. *J. Biol. Chem.* **277:** 8267–8272.
14. Miyoshi, H., J. W. Perfield, II, S. C. Souza, W-J. Shen, H-H. Zhang, Z. S. Stancheva, F. B. Kraemer, M. S. Obin, and A. S. Greenberg. 2007. Control of adipose triglyceride lipase action by serine 517 of perilipin A globally regulates protein kinase A-stimulated lipolysis in adipocytes. *J. Biol. Chem.* **282:** 996–1002.
15. Zimmermann, R., J. G. Strauss, G. Haemmerle, G. Schoiswohl, R. Birner-Gruenberger, M. Riederer, A. Lass, G. Neuberger, F. Eisenhaber, A. Hermetter, et al. 2004. Fat mobilization in adipose tissue is promoted by adipose triglyceride lipase. *Science.* **306:** 1383–1386.
16. Zhang, H. H., S. C. Souza, K. V. Muliro, F. B. Kraemer, M. S. Obin, and A. S. Greenberg. 2003. Lipase-selective functional domains of perilipin A differentially regulate constitutive and protein kinase A-stimulated lipolysis. *J. Biol. Chem.* **278:** 51535–51542.
17. Miyoshi, H., S. C. Souza, H. H. Zhang, K. J. Strissel, M. A. Christoffolete, J. Kovsan, A. Rudich, F. B. Kraemer, A. C. Bianco, M. S. Obin, et al. 2006. Perilipin promotes hormone-sensitive lipase-mediated adipocyte lipolysis via phosphorylation-dependent and -independent mechanisms. *J. Biol. Chem.* **281:** 15837–15844.
18. Tansey, J. T., A. M. Huml, R. Vogt, K. E. Davis, J. M. Jones, K. A. Fraser, D. L. Brasaemle, A. R. Kimmel, and C. Londos. 2003. Functional studies on native and mutated forms of perilipins. A role in protein kinase A-mediated lipolysis of triacylglycerols. *J. Biol. Chem.* **278:** 8401–8406.
19. Garcia, A., V. Subramanian, A. Sekowski, S. Bhattacharyya, M. W. Love, and D. L. Brasaemle. 2004. The amino and carboxyl termini of perilipin A facilitate the storage of triacylglycerols. *J. Biol. Chem.* **279:** 8409–8416.
20. Subramanian, V., A. Garcia, A. Sekowski, and D. L. Brasaemle. 2004. Hydrophobic sequences target and anchor perilipin A to lipid droplets. *J. Lipid Res.* **45:** 1983–1991.
21. Subramanian, V., A. Rothenberg, C. Gomez, A. W. Cohen, A. Garcia, S. Bhattacharyya, L. Shapiro, G. Dolios, R. Wang, M. P. Lisanti, et al. 2004. Perilipin A mediates the reversible binding of CGI-58 to lipid droplets in 3T3-L1 adipocytes. *J. Biol. Chem.* **279:** 42062–42071.
22. Soloveva, V., R. A. Graves, M. M. Rasenick, B. M. Spiegelman, and S. R. Ross. 1997. Transgenic mice overexpressing the beta 1-adrenergic receptor in adipose tissue are resistant to obesity. *Mol. Endocrinol.* **11:** 27–38.
23. Rickwood, D., M.T. Wilson, and V. M. Darley-Usmar. 1988. Isolation and characteristics of intact mitochondria. *In* Mitochondria: A Practical Approach. IRL Press, Oxford, UK. 1–16.
24. Ribeiro, M. O., S. D. Carvalho, J. J. Schultz, G. Chiellini, T. S. Scanlan, A. C. Bianco, and G. A. Brent. 2001. Thyroid hormone-sympathetic interaction and adaptive thermogenesis are thyroid hormone receptor isoform-specific. *J. Clin. Invest.* **108:** 97–105.
25. Souza, S. C., M. Yamamoto, M. Franciosa, P. Lien, and A. Greenberg. 1998. BRL blocks the lipolytic actions of tumor necrosis factor-alpha (TNF-α): a potential new insulin-sensitizing mechanism for the thiazolidinediones. *Diabetes.* **47:** 691–695.
26. de Jesus, L. A., S. D. Carvalho, M. O. Ribeiro, M. Schneider, S. W. Kim, J. W. Harney, P. R. Larsen, and A. C. Bianco. 2001. The type 2 iodothyronine deiodinase is essential for adaptive thermogenesis in brown adipose tissue. *J. Clin. Invest.* **108:** 1379–1385.
27. Livak, K. J., and T. D. Schmittgen. 2001. Analysis of relative gene expression data using real-time quantitative PCR and the 2(-Delta Delta C(T)) method. *Methods.* **25:** 402–408.
28. Tansey, J., C. Sztalryd, J. Gruia-Gray, D. Roush, J. Zeo, O. Gavrilova, M. Reitman, C-X. Deng, C. Ki, A. Kimmel, and C. Londos. 2001. Perilipin ablation results in a lean mouse with aberrant adipocyte lipolysis, enhanced leptin production, and resistance to diet-induced obesity. *Proc. Natl. Acad. Sci. USA.* **98:** 6494–6499.
29. Krauss, S., C. Y. Zhang, and B. B. Lowell. 2005. The mitochondrial uncoupling-protein homologues. *Nat. Rev. Mol. Cell Biol.* **6:** 248–261.
30. Martinez-Botas, J., J. Andreson, D. Tessler, A. Lapillojnne, B. H-J. Chang, M. Quast, D. Gorenstein, K-H. Chen, and L. Chan. 2000. Absence of perilipin results in leanness and reverses obesity in Leprdb/db mice. *Nat. Genet.* **26:** 474–479.